

# Slow light enhancement of nonlinear effects in silicon engineered photonic crystal waveguides

Christelle Monat,<sup>1,\*</sup> Bill Corcoran,<sup>1</sup> Majid Ebnali-Heidari,<sup>1</sup> Christian Grillet,<sup>1</sup> Benjamin J. Eggleton,<sup>1</sup> Thomas P. White,<sup>2</sup> Liam O'Faolain,<sup>2</sup> and Thomas F. Krauss<sup>2</sup>.

<sup>1</sup> Institute of Photonics and Optical Science (IPOS), Centre for Ultrahigh-bandwidth Devices for Optical Systems (CUDOS), School of Physics, NSW 2006, Australia

<sup>2</sup> School of Physics and Astronomy, University of St Andrews, St Andrews, Fife, KY16 9SS, UK.

\*Corresponding author: [monat@physics.usyd.edu.au](mailto:monat@physics.usyd.edu.au)

**Abstract:** We report nonlinear measurements on 80 $\mu$ m silicon photonic crystal waveguides that are designed to support dispersionless slow light with group velocities between  $c/20$  and  $c/50$ . By launching picosecond pulses into the waveguides and comparing their output spectral signatures, we show how self phase modulation induced spectral broadening is enhanced due to slow light. Comparison of the measurements and numerical simulations of the pulse propagation elucidates the contribution of the various effects that determine the output pulse shape and the waveguide transfer function. In particular, both experimental and simulated results highlight the significant role of two photon absorption and free carriers in the silicon waveguides and their reinforcement in the slow light regime.

©2009 Optical Society of America

**OCIS codes:** (130.5296) Photonic crystal waveguides; (190.4390) Nonlinear optics, integrated optics

---

## References and links

1. T. Baba, "Slow light in photonic crystals," *Nature Photon.* **2**, 465-473 (2008).
2. M. Soljacic, S. G. Johnson, S. H. Fan, M. Ibanescu, E. and J. D. Joannopoulos, "Photonic-crystal slow-light enhancement of nonlinear phase sensitivity," *J. Opt. Soc. Am. B-Opt. Phys.* **19**, 2052-2059 (2002).
3. Y. A. Vlasov, M. O'Boyle, H. F. Hamann and S. J. McNab, "Active control of slow light on a chip with photonic crystal waveguides," *Nature* **438**, 65-69 (2005).
4. E. Drouard, H. Hattori, C. Grillet, A. Kazmierczak, X. Letartre, P. Rojo-Romeo, and P. Viktorovitch, "Directional channel-drop filter based on a slow Bloch mode photonic crystal waveguide section," *Opt. Express* **13**, 3037-3048 (2005).
5. T.F. Krauss, "Why do we need slow light?," *Nature Photon.* **2**, 448-449 (2008).
6. T. F. Krauss, "Slow light in photonic crystal waveguides," *J. Phys. D-Appl. Phys.* **40**, 2666-2670 (2007).
7. M. D. Settle, R. J. P. Engelen, M. Salib, A. Michaeli, L. Kuipers, and T. F. Krauss, "Flatband slow light in photonic crystals featuring spatial pulse compression and terahertz bandwidth," *Opt. Express* **15**, 219-226 (2007).
8. S. Hughes, L. Ramunno, J. F. Young, and J. E. Sipe, "Extrinsic optical scattering loss in photonic crystal waveguides: role of fabrication disorder and photon group velocity," *Phys. Rev. Lett.* **94**, 0339031-0339034 (2005).
9. L. C. Andreani, and D. Gerace, "Light-matter interaction in photonic crystal slabs," *Phys. Status Solidi B* **244**, 3528-3539 (2007).
10. R. J. P. Engelen, Y. Sugimoto, Y. Watanabe, J. P. Korterik, N. Ikeda, N. F. van Hulst, K. Asakawa, and L. Kuipers, "The effect of higher-order dispersion on slow light propagation in photonic crystal waveguides," *Opt. Express* **14**, 1658-1672 (2006).
11. X. Letartre, C. Seassal, C. Grillet, P. Rojo-Romeo, P. Viktorovitch, M. L. d'Yerville, D. Cassagne, and C. Jouanin, "Group velocity and propagation losses measurement in a single-line photonic-crystal waveguide on InP membranes," *Appl. Phys. Lett.* **79**, 2312-2314 (2001).
12. M. Notomi, K. Yamada, A. Shinya, J. Takahashi, C. Takahashi, and I. Yokohama, "Extremely large group-velocity dispersion of line-defect waveguides in photonic crystal slabs," *Phys. Rev. Lett.* **87**, 2539021-2539024 (2001).
13. H. Oda, K. Inoue, Y. Tanaka, N. Ikeda, Y. Sugimoto, H. Ishikawa, and K. Asakawa, "Self-phase modulation in photonic-crystal-slab line-defect waveguides," *Appl. Phys. Lett.* **90**, 231102 (2007).

14. H. Oda, K. Inoue, A. Yamanaka, N. Ikeda, Y. Sugimoto, and K. Asakawa, "Light amplification by stimulated Raman scattering in AlGaAs-based photonic-crystal line-defect waveguides," *Appl. Phys. Lett.* **93**, 051114 (2008).
15. L. H. Frandsen, A. V. Lavrinenko, J. Fage-Pedersen, and P. I. Borel, "Photonic crystal waveguides with semi-slow light and tailored dispersion properties," *Opt. Express* **14**, 9444-9450 (2006).
16. S. Kubo, D. Mori, and T. Baba, "Low-group-velocity and low-dispersion slow light in photonic crystal waveguides," *Opt. Lett.* **32**, 2981-2983 (2007).
17. J. Li, T. P. White, L. O. Faolain, A. Gomez-Iglesias, and T. F. Krauss, "Systematic design of flat band slow light in photonic crystal waveguides," *Opt. Express* **16**, 6227-6232 (2008).
18. L. O'Faolain, X. Yuan, D. McIntyre, S. Thoms, H. Chong, R. M. De la Rue, and T. F. Krauss, "Low-loss propagation in photonic crystal waveguides," *Electron Lett.* **42**, 1454-1455 (2006).
19. J. P. Hugonin, P. Lalanne, T. P. White, and T. E. Krauss, "Coupling into slow-mode photonic crystal waveguides," *Opt. Lett.* **32**, 2638-2640 (2007).
20. A. Gomez-Iglesias, D. O'Brien, L. O'Faolain, A. Miller, and T. F. Krauss, "Direct measurement of the group index of photonic crystal waveguides via Fourier transform spectral interferometry," *Appl. Phys. Lett.* **90**, 261107 (2007).
21. L. H. Yin and G. P. Agrawal "Impact of two-photon absorption on self-phase modulation in silicon waveguides," *Opt. Lett.* **32**, 2031-2033 (2007).
22. N. A. R. Bhat, and J. E. Sipe, "Optical pulse propagation in nonlinear photonic crystals," *Phys. Rev. E* **64**, 0566041-05660416 (2001).
23. M. Dinu, F. Quochi, and H. Garcia, "Third-order nonlinearities in silicon at telecom wavelengths," *Appl. Phys. Lett.* **82**, 2954-2956 (2003).
24. N. Le Thomas, R. Houdré, L. H. Frandsen, J. Fage-Pedersen, A. Lavrinenko, and P. I. Borel, "Grating-assisted superresolution of slow waves in Fourier space," *Phys. Rev. B* **76**, 035103 (2007).
25. R. J. P. Engelen, D. Mori, T. Baba, and L. Kuipers, "Two regimes of slow light losses revealed by adiabatic reduction of group velocity" *Phys. Rev. Lett.* **101**, 103901 (2008).
26. V. G. Ta'eed, M. Shokooh-Saremi, L. Fu, I. C. M. Littler, D. J. Moss, M. Rochette, B. J. Eggleton, Y. Ruan, and B. Luther-Davies, "Self-phase modulation-based integrated optical regeneration in chalcogenide waveguides," *IEEE J. Sel. Top. Quantum. Electron.* **12**, 360-370 (2006).
27. M. Gnan, S. Thoms, D. S. Macintyre, R. M. De La Rue, and M. Sorel, "Fabrication of low-loss photonic wires in silicon-on-insulator using hydrogen silsequioxane electron-beam resist," *Electron. Lett.* **44**, 115-116 (2008).
28. W. Ding, C. Benton, A. V. Gorbach, W. J. Wadsworth, J. C. Knight, D. V. Skryabin, M. Gnan, M. Sorel, and R. M. De La Rue, "Solitons and spectral broadening in long silicon-on-insulator photonic wires," *Opt. Express* **16**, 3310-3319 (2008).

## 1. Introduction

In recent years, there has been a growing interest in slow light in photonic crystals (PhC) [1], both in the context of optical delay lines but also for realizing compact optical functions [2-4] and more generally for nonlinear photonics [5]. It is expected that slow light will allow for a reduction of either the power or the physical length needed to observe the same linear or nonlinear effects as in the fast light regime [2]. In particular, theoretical studies have predicted a quadratic enhancement of nonlinear effects due to slow light. This is based on both the longer time that the slow light spends to travel a given physical distance, and on the increase of the slow light energy density due to the spatial pulse compression, both effects increasing the interaction between light and the nonlinear material [6,7]. So far, however, such nonlinear enhancement has not been systematically and unambiguously observed and studied. One reason is that slow light structures also suffer generally from the simultaneous enhancement of linear propagation losses [8,9], large coupling losses, as well as significant higher order dispersion [10].

Planar PhC waveguides, which combine a periodic lattice of air holes and a vertical step index waveguide, offer a unique platform to engineer the dispersion properties of light at the micrometer scale [1]. This architecture has proven to be effective and flexible to control both the speed of light and its associated dispersion on-chip. The last point is crucial for nonlinear optics as the large dispersion that is typically associated to slow light modes [11,12] tends to dramatically distort and stretch the slow light pulses, thereby compromising the benefits of spatial pulse compression provided by slow light [10]. Such a large dispersion has restricted the demonstration of nonlinear effects –such as stimulated Raman scattering or Self Phase Modulation (SPM)– in standard W1 PhC waveguides to the fast light regime and using long

(~1mm) waveguides [13,14]. Very recently, several approaches have been successfully investigated to engineer the dispersion of slow light modes and to optimize the bandwidth-delay product in planar PhC waveguides [15-17]. These efforts make it now possible to implement slow light in practical nonlinear functions.

Here, as an example of a slow light enhanced nonlinear effect, we report the experimental observation of slow light enhanced SPM exhibited by picosecond-pulses propagating through silicon PhC waveguides as short as 80  $\mu\text{m}$ . This demonstration has been made possible due to the careful engineering of the PhC geometry which provides us with a series of waveguides with (i) a controlled low group velocity ranging between  $c/20$  and  $c/50$  and (ii) a limited group velocity dispersion associated to the slow light regime over at least 5nm bandwidth for all of the guides. The experimental results are supported by Split-Step-Fourier-Method (SSFM) modelling, including Two Photon Absorption (TPA) and free carrier (FC) effects in silicon, which gives further insight into the various contributions of these effects to both the output pulse signature and the power transfer function. In particular, both experiment and simulation highlight the reinforcement of TPA and FC effects in the slow light regime.

## 2. Dispersionless slow light PhC waveguides

The PhC waveguides were fabricated on a SOITEC silicon-on-insulator wafer comprising a 220 nm thick silicon layer on 2  $\mu\text{m}$  layer of silica using electron-beam lithography and reactive ion etching [17,18]. The total length of the waveguide structure is 0.9mm; it comprises an 80  $\mu\text{m}$  long suspended silicon PhC waveguide and 0.4 mm long, 3 $\mu\text{m}$  wide ridge access waveguides on each side that are tapered down to 0.7  $\mu\text{m}$  wide ridges close to the PhC section (see Fig. 1(a)). The PhC waveguides consist of a triangular lattice of air holes with a period  $a$  of ~410 nm, and hole radii of  $\sim 0.29a$ , where one row of holes has been omitted along the  $\Gamma\text{K}$  direction (Fig 1(b)). To enhance coupling from the access ridges into the slow light PhC waveguide, an intermediate region consisting of ten periods of PhC waveguide with a “stretched” lattice of period ~440 nm was added at either end of the slow light section [19].

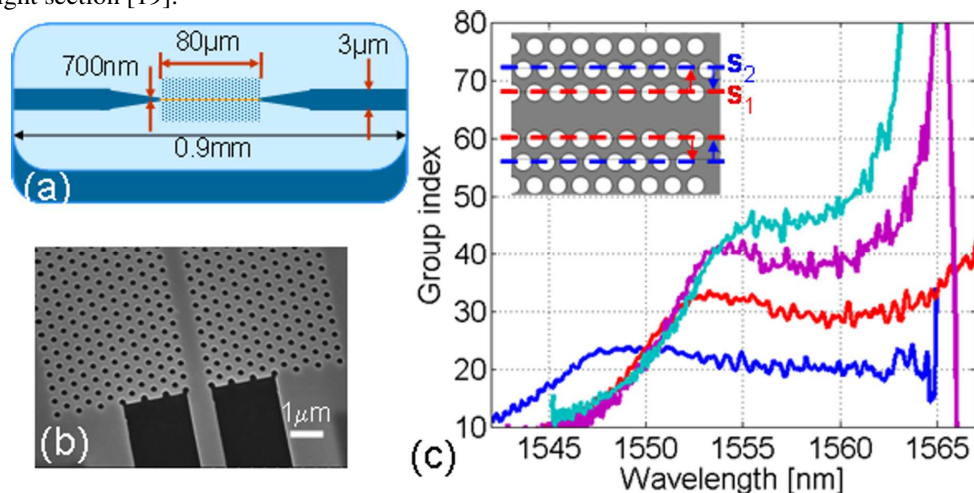


Fig. 1. (a) Schematic of the silicon waveguide with the 80 $\mu\text{m}$  PhC waveguide in the middle. (b) Scanning electron microscope image of a silicon PhC waveguide connected to the tapered ridge access waveguide. (c) Measured group index dispersion of the four engineered PhC waveguides (see Table 1). The inset shows the principle of the engineered PhC waveguide design where the two first rows of holes are shifted toward or away from the waveguide axis.

The PhC waveguides have been engineered so that they display a slow group velocity with low dispersion over a substantial bandwidth (>5nm). This is achieved by appropriately shifting the position of the first two rows of holes adjacent to the centre of the W1 PhC waveguide, as represented in the inset of Fig. 1(c) [17]. Using this approach, optimised shift

parameters have been identified for targeting specific group indices [17]. Figure 1(c) shows the group index dispersion associated to the fundamental mode of the resulting engineered PhC waveguides, as measured experimentally [20]. These curves all present a spectral window where the group index ( $n_g$ ) is nearly constant over at least 5nm, while the corresponding group velocities range between  $c/20$  and  $c/50$ . These dispersionless slow light PhC waveguides have been fabricated using the parameters summarized in Table 1. Note that the lattice period is also varied so that the low dispersion region of each waveguide occurs around the same wavelength.

Table 1. Summary of the parameters of the four dispersion engineered PhC waveguides that are optimized for displaying a dispersionless slow light propagation window. The positive and negative shifts indicated correspond to a displacement perpendicular to the waveguide direction, away from the waveguide axis and toward it, respectively.

Period	1 <sup>st</sup> row shift $s_1$	2 <sup>nd</sup> row shift $s_2$	Group index
406nm	56nm	16nm	~20
408nm	52nm	0nm	~30
410nm	50nm	-10nm	~40
410nm	48nm	-16nm	~50

### 3. Modelling of the pulse propagation across silicon PhC structures

We use the following nonlinear Schrödinger equation to simulate the evolution of the slowly varying envelope  $A(z,T)$  of the pulse electric field amplitude as it propagates through the waveguide [21]:

$$\frac{\partial A}{\partial z} + \frac{\alpha}{2} A + \frac{i\beta_2}{2} \frac{\partial^2 A}{\partial T^2} - \frac{\beta_3}{6} \frac{\partial^3 A}{\partial T^3} = i\gamma(|A|^2 A) - \frac{\beta_{TPA}}{2A_{eff}} |A|^2 A - N_c \left( \frac{\sigma}{2} + \frac{2k_c i\pi}{\lambda_0} \right) A \quad (1)$$

In this equation, the second, third, and fourth term on the left hand side describe the linear propagation loss, and the second and third order dispersion. The first term on the right hand side of Eq. (1) describes the nonlinear Kerr effect using the nonlinear parameter  $\gamma$  (equal to  $2\pi n_2 / [\lambda_0 A_{eff}]$  with  $n_2$  being the Kerr coefficient of silicon,  $\lambda_0$  the central wavelength of the pulse and  $A_{eff}$  the cross-section area of the PhC mode). The second and last term are related to TPA and FC effects respectively. Two terms describe the interaction with the FCs (of density  $N_c$ ) as both an additional source of absorption (accounted for by the  $\sigma$  parameter) and dispersion (accounted for by  $k_c$ ) from the FC dependence of the silicon refractive index.

In silicon, FCs are generated through TPA, following the equation [21]

$$\frac{\partial N_c(t)}{\partial t} = \frac{\beta_{TPA}}{2h\nu_0 A_{eff}^2} |A|^4 - \frac{N_c}{\tau_{recomb}} \quad (2)$$

where  $\tau_{recomb}$  corresponds to the FC lifetime in silicon. Although the latter is reduced in silicon PhCs due to their large surface to volume ratio, the FC lifetime is long enough (typically a few hundreds of picoseconds) that we can neglect FC recombination within the picosecond duration of the probe pulses. In addition, since the time between subsequent pulses is long (~250ns) compared to  $\tau_{recomb}$ , we neglect FC accumulation over subsequent pulses. These two assumptions allow us to drop the second term on the right hand side of Equation (2) and calculate  $N_c(t)$  by integrating the TPA induced FC generation term over the pulse duration.

We introduce the modal group velocity into Equation (1) by replacing  $\alpha$ ,  $\gamma$ ,  $\beta_{TPA}$ ,  $\sigma$  and  $k_c$  by  $\alpha \times S$ ,  $\gamma \times S^2$ ,  $\beta_{TPA} \times S^2$ ,  $\sigma \times S$  and  $k_c \times S$ , respectively, where  $S$  represents a slow-down factor equal to the ratio of the group index  $n_g$  over the silicon refractive index  $n_{Si}$ . The

quadratic dependence of the nonlinear coefficients  $\gamma$  and  $\beta_{TPA}$  with  $S$  is based on theoretical derivations such as in Ref [22].

Equation (1) is solved using the SSFM with the values for the various silicon parameters as summarized in Table 2. This gives both the temporal and spectral shape of the pulse as it propagates through the structure. This modelling allows us to understand the relative contributions of dispersion, TPA and FCs on the spectral change of the pulse. It therefore provides us with a useful tool to analyse and compare the experimental results of section 4. Conversely, the respective  $S$ -dependences of the various coefficients are validated by the agreement obtained with the experimental results.

Table 2. Summary of the parameters used in Equations (1) and (2) for silicon around 1550nm, mostly from [21] and [23].

$n_2$ Kerr coefficient	$\beta_{TPA}$ TPA coefficient	$\sigma$ FC absorption cross-section	$k_c$ FC dispersion coefficient	$\alpha$ PhC propagation loss
$5 \times 10^{-18} \text{ m}^2/\text{W}$	$1 \times 10^{-11} \text{ m/W}$	$1.45 \times 10^{-21} \text{ m}^2$	$1.35 \times 10^{-27} \text{ m}^3$	20 dB/cm

#### 4. Experimental and simulation results

The nonlinear measurements are performed using a figure-of-8 passive mode-locked laser that generates close to transform-limited 1.2 ps pulses at a 4 MHz repetition rate. The laser is tunable over the C-band so that the different waveguides can be probed in their slow light dispersionless regime around 1555nm. The input polarisation of the pulses is controlled to excite primarily the TE-like modes in the waveguides. We couple the light in and out of the waveguides using lensed fibers with a 2.5  $\mu\text{m}$  spot diameter, providing a total insertion loss of about 15 dB. The spectra are monitored for various input powers using an optical spectrum analyser.

We first probe two reference waveguides. The first one is a 0.9mm long, 3 $\mu\text{m}$  wide ridge waveguide –similar to the access ridges. The second reference comprises an 80  $\mu\text{m}$  long, 0.7 $\mu\text{m}$  wide nanowire that is similar to the tapered ridges directly surrounding the PhC section; it includes on both sides the same tapered access ridge waveguides as the PhC waveguides, therefore providing a reference fast waveguide with the same degree of optical confinement as the PhC waveguide. Figures 2(a-b) show the transmission spectra obtained while varying the input peak power between 2 W and 235 W. The actual peak power coupled inside the structures is estimated to be ~20% of these values. The output pulse is spectrally broadened for increasing power as a signature of the SPM experienced by the 1.2ps pulses across both reference waveguides. Note the slightly broader effect through the nanowire reference though, as expected due to its stronger optical confinement.

Figures 2 (c-f) show the equivalent spectra obtained when probing the four slow light waveguides with group velocities ranging between  $c/20$  and  $c/50$  (see Table 1). These spectra exhibit much greater SPM-induced spectral broadening with increasing power than either of the two reference structures. This clearly demonstrates the dominant contribution of the 80 $\mu\text{m}$  slow PhC waveguides to the output spectral signatures observed in Figs 2(c-f). Most importantly, the spectral broadening through the slow light waveguides increases with the waveguide group index. Note that this slow light enhanced spectral broadening is more striking at lower coupled powers (7.5W or 15W for instance). In addition, the pulse spectra associated to the PhC waveguides become both asymmetric and strongly blue-shifted when increasing the input power and the waveguide group index.

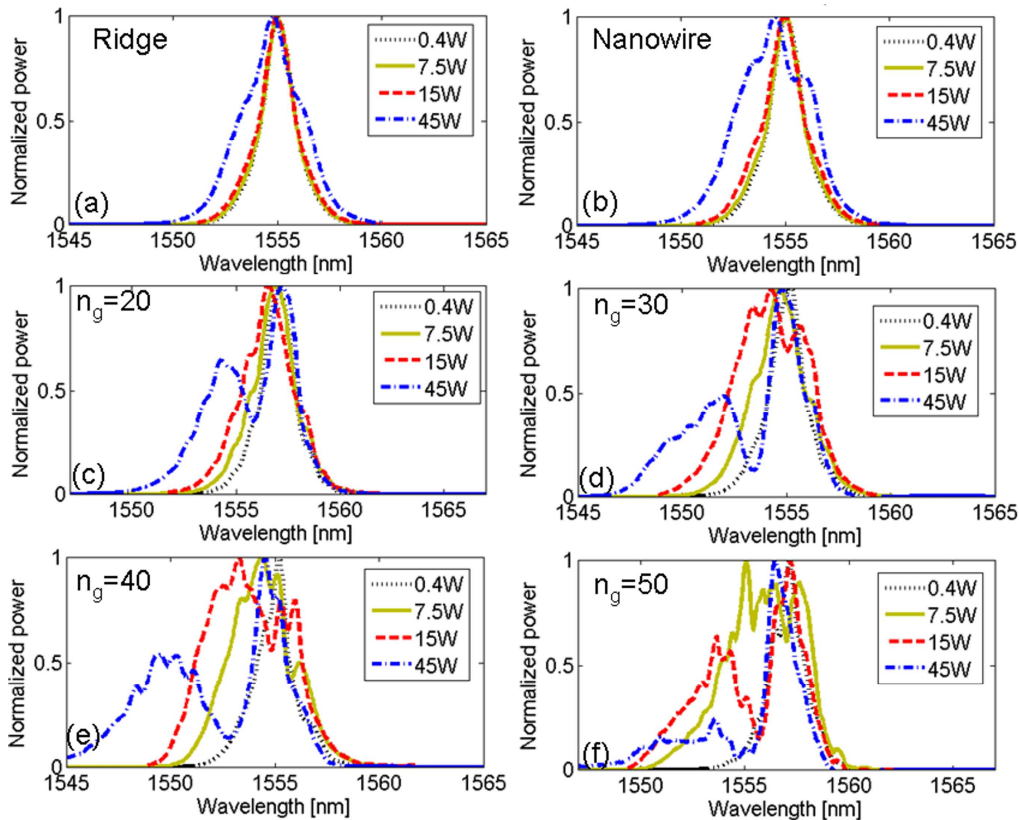


Fig. 2. Output spectra at different coupled powers of 1.2ps pulses propagating through the reference ridge waveguide (a), the reference 80  $\mu\text{m}$  long nanowire (b) and the slow waveguides with group indices between 20 and 50 (c-f).

The spectral signatures of the slow light waveguides can be reproduced with reasonable agreement using the SSFM that solves the Eq. (1) and (2). We consider for these calculations PhC waveguides with zero dispersion and surrounded by two access ridge waveguides. Three of these plots are displayed in Figs 3 (d-f) along with the corresponding experimental data (a-c) for the slow light waveguides with group indices of 30, 40 and 50. The 2D plots in Fig. 3 map the output pulse spectra with the wavelength on the horizontal axis and the input power increasing along the vertical axis. These plots highlight that the rate at which the spectrum broadens with power is larger for slower waveguides, while the experimental spectral shapes agree reasonably well with the calculated ones. Both experiment and simulations also show an enhanced blue-shift for slower guides; this is due, as explained below, to the increased interaction with the FCs. However, we note the peculiar signature for the slowest waveguide in Fig. 3(c): the spectrum strongly broadens for low peak powers but the short wavelengths that are generated early dissipate for higher powers with a much larger effect than what is expected from the modelling. Although no convincing explanation has yet been found, it may be possible to attribute this to the lower bandwidth associated to the dispersionless window of this waveguide. This may result in a walk-off phenomenon between the slow light pulse and the frequency shifted components that travel at faster group velocities. It may also be related to some localization effects [24] or irregular behaviour [25] that have been observed at low group velocities.

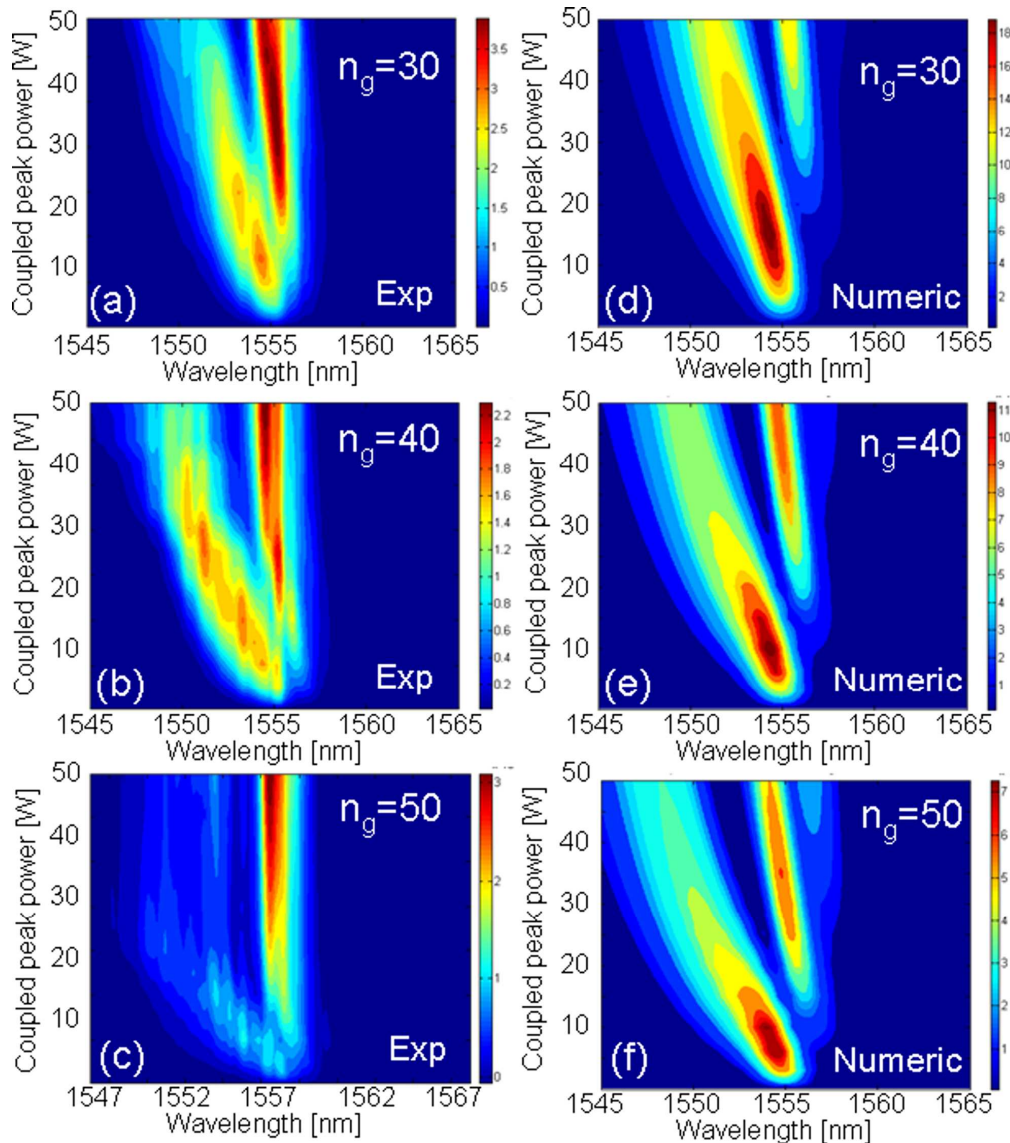


Fig. 3. 2D plots showing the output pulse spectra versus coupled peak power for 3 slow light waveguides with a group index of 30 (a,d), 40 (b,e) and 50 (c,f) as measured experimentally (a-c) and calculated using the SSFM (d-f).

The modelling allows us to separate the different contributions from the Kerr effect and the FC dispersion to the pulse spectral signature. The first effect induces a symmetric spectral broadening of the pulse. By contrast, the second one, which also contributes to the spectral broadening (see section 5), is responsible for an additional and overall blue-shift of the pulse spectrum, as observed in Figs (2-3). This can be explained qualitatively as a result of the gradual FC density increase across the pulse and the fact that the silicon refractive index depends inversely on the FC density. This creates an asymmetric and positive frequency chirp across the pulse that manifests as the generation of blue shifted frequency components [21]. To illustrate the slow light dependence of this effect, Fig 4(a) shows the averaged wavelength of the output pulses plotted as a function of the waveguide group index, as measured and calculated for 15W coupled peak power. Whereas this value remains zero in the absence of

FCs, the blue-shift increases with  $n_g$ , showing that the FC dispersion effect is enhanced due to slow light.

The group velocity also significantly affects the power transfer function, as shown in Fig 4(b). Good agreement is obtained with the simulated results using the values in Table 2. We observe that (i) a strong saturation effect occurs at high input powers for the slow light waveguides and (ii) the clamping arises for lower input powers when increasing the waveguide group index. This confirms the slow light enhancement of the nonlinear loss, which was accounted for in the simulations, by the  $S^2$ - and  $S$ -dependence of  $\beta_{TPA}$  (TPA) and  $\sigma$  (FC absorption) respectively. The calculations also indicate that the nonlinear losses at high powers are due almost equally to TPA and TPA-induced FC absorption. In addition, these plots tend to validate the assumption of an  $S$ -dependent linear propagation loss in these engineered PhC waveguides (as opposed to the  $S^2$  dependence in typical W1 PhC waveguides near the cut-off [8]).

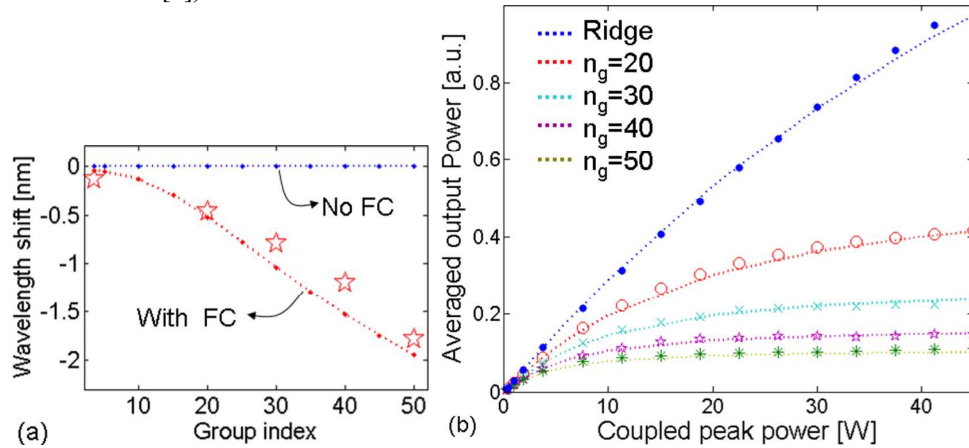


Fig. 4. (a) Spectral shift of the averaged wavelength of the output pulses versus group index (including the reference nanowire) for a coupled peak power of 15W, from both experiments (red stars) and simulations (dotted red line). The blue dotted line represents the calculated shift in the absence of free carriers. (b) Average output power versus coupled peak power for the different waveguides as derived from the measurements (dots) and the simulations (dotted lines).

## 5. Analysis and discussion

The results in the previous section show that several effects are enhanced simultaneously in the slow light regime, namely the linear propagation loss, the Kerr effect, TPA, and the interaction with TPA induced FCs. FC effects, particularly important in silicon due to its relatively high TPA, manifest as an additional nonlinear loss term (see Fig. 4(b)) as well as in the blue-shift associated with the FC density increase across the picosecond pulse (Fig. 4(a)). In silicon, FC effects are doubly enhanced in the slow light regime due to their enhanced creation through TPA ( $\propto S^2$ ) and, subsequently, their enhanced interaction ( $\propto S$ ) with the slowly propagating light. The modelling allows us to identify the different contributions to the pulse spectral behaviour and transfer function, while the good agreement with the experimental results validates the  $S$ -dependences assumed for the various effects.

The experimental and numerical spectral broadening versus input power are all summarized in Fig. 5(a-b) for the different waveguides using as an indicator the averaged deviation of the pulse spectrum,  $\langle |\lambda - \lambda_0| \rangle$ , from the input wavelength,  $\lambda_0$ . These curves quantify the nonlinear spectral broadening enhancement obtained when increasing the group index of the waveguide. The peculiar experimental signature of the slowest waveguide, which was mentioned above, is visible through the roll-off behaviour of the  $n_g=50$  waveguide at high power that deviates from the modelling. It is worth pointing out that the curves from the modelling tend to the same and lower broadening rate at high input powers, regardless of the

group index. This can be inferred separately from an analytical derivation of the nonlinear phase shift in the presence of TPA. Therefore, even theoretically, the maximum  $n_g$ -enhancement is obtained at relatively low powers. These curves also reveal that conversely, the input power needed to obtain a targeted spectral broadening is strongly reduced by using slower PhC waveguides. For instance, to double the spectral bandwidth of the pulse through SPM, the coupled peak power is reduced from 50 W to  $\sim 8$ W, i.e. by almost a factor 7, by decreasing the group velocity from  $c/3$  to  $c/50$ .

It is remarkable that despite the simultaneous slow light increase of linear and nonlinear propagation losses, we still get a net enhancement of the spectral broadening in the slow light regime. For instance, as highlighted on Fig 5(c), the spectral broadening increases by a factor of 2.8 at 15W coupled peak power. Note that although moderate, this value is close to the factor 3 predicted numerically for perfectly zero-dispersion slow light PhC waveguides (see Fig. 5(c)), confirming the actual low dispersion of the engineered PhC waveguides investigated here. Figure 5(c) shows that this enhancement is reduced by the slow light enhanced TPA and FC absorption, since the calculated broadening factor is more than 5 in the absence of any nonlinear (TPA or FC) loss terms. These results suggest that the use of alternative materials with lower TPA should therefore provide a larger slow light enhancement of the Kerr induced SPM signature. However, the simulated results with TPA but no FCs give a lower spectral broadening  $n_g$ -enhancement ( $\times 2$ ) than with both loss terms. This highlights the contribution of the FCs to the spectral broadening of the pulse, the interest of which will be tempered for fast optical signal processing applications due to their slower dynamics as compared to the pure Kerr nonlinearity.

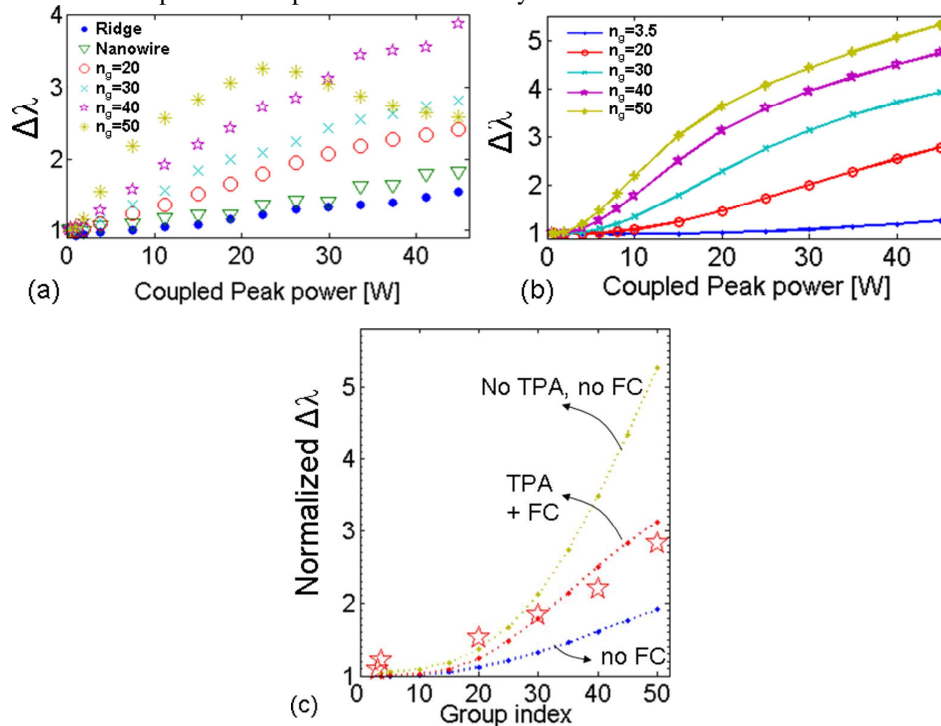


Fig. 5. (a) Averaged spectral broadening  $\Delta\lambda = \langle |\lambda - \lambda_0| \rangle$  of the output pulse versus coupled peak power as measured experimentally for the series of waveguides on Fig 2. The values are normalized to the spectral broadening of the pulse at low power. (b) Equivalent figures from the calculations. (c) Normalized averaged spectral broadening  $\langle |\lambda - \lambda_0| \rangle$  versus group index from both experiments (red stars) and the simulations (dotted lines) in the presence of both TPA and FCs (red line), only TPA (blue line) and no TPA nor FCs (brown line).

In addition to being of fundamental interest to verify experimentally the slow light dependence of nonlinear effects, this study opens new opportunities in terms of the realization of optical nonlinear functions with better performance based on slow light PhC waveguides. For instance, exploiting the SPM induced spectral broadening has been suggested for realizing optical regenerators [26]. The results above suggest that such devices could be realized from compact (80 $\mu\text{m}$ ) PhC waveguides. More generally, it is worth looking more closely at the length scales involved in these engineered slow PhC waveguides to clarify the regime where the performance of slow light based nonlinear functions would out-perform their fast light counterparts. The reduction of the dispersion to  $\sim 1.10^{-21} \text{ s}^2/\text{m}$  gives an associated dispersion length as large as 1mm in the picosecond regime. This is therefore not the limiting factor for exploiting long devices that generally provide larger nonlinear effects. The estimated PhC propagation loss  $\alpha$  ( $\sim 20\text{dB}/\text{cm}$ ) and its linear  $S$ -dependence give an associated effective length ( $L_{\text{eff}}=(1-\exp(-\alpha\times L))/\alpha$ ) bounded to a maximum value ( $=1/\alpha$ ) of 2mm for a fast waveguide and only 150  $\mu\text{m}$  for a  $n_g=50$  waveguide. Note that this value is further increased to above 4cm for “fast” nanowire silicon waveguides providing the same degree of optical confinement due to the extra low-loss ( $<1\text{dB}/\text{cm}$ ) values reported for the mature nanowire fabrication technology [27-28]. Hence, the performance of long slow light PhC waveguides will be penalized compared to fast PhC waveguides or silicon nanowires. By contrast, the effective length of 80 $\mu\text{m}$  long waveguides is only slightly reduced from 78 $\mu\text{m}$  (80  $\mu\text{m}$ ) for a fast PhC waveguide (nanowire) to 62  $\mu\text{m}$  for a  $n_g=50$  PhC waveguide. This reemphasizes the potential interest of slow light PhC silicon waveguides as a basis for relatively low power *and* compact nonlinear devices, while revealing that the effectiveness of long, slow PhC waveguides is limited by loss, at least with the present technology.

## 6. Conclusion

In conclusion, we have thoroughly investigated the nonlinear effects undergone by picosecond-pulses propagating through different 80  $\mu\text{m}$  long silicon PhC waveguides with group velocities ranging between  $c/20$  and  $c/50$ . The comparison of the respective output spectral signatures through fast and slow waveguides reveals an enhancement of the SPM induced spectral broadening ( $\times 2.8$  at 15W coupled power). Conversely, we also show a reduction in the input power (by more than a factor of 6) needed to double the pulse spectral bandwidth by using a slow ( $c/50$ ) waveguide. The observed enhancement is however reduced by the simultaneous reinforcement of TPA and FCs in the slow light regime, as attested by both the output power saturation and the increased blue shift of the pulses arising from slower waveguides. The experimental results are well supported by SSFM simulations, enabling us to evaluate the respective contributions of the Kerr effect, TPA and FCs in the slow light regime, and to identify the potential of slow light Si PhC waveguides for compact nonlinear functions.

## Acknowledgments

The support of the Australian Research Council through its Federation Fellow, Centre of Excellence and Discovery Grant programs is gratefully acknowledged. Additional acknowledgement is given to the support of the School of Physics, University of Sydney, through its Denison Foundation and the International Science Linkages program of the Department of Education, Science and Technology. The silicon samples were fabricated in the framework of the EU-FP6 funded ePIXnet Nanostructuring Platform for Photonic Integration ([www.nanophotonics.eu](http://www.nanophotonics.eu)). T.P. White acknowledges the support of the EU-FP6 Marie Curie Fellowship “SLIPPRY”. M. Ebnali-Heidari acknowledges the support of the Iran Telecommunication Research Center (ITRC).